JOBNAME: jcfs 17#1 2006 PAGE: 1 OUTPUT: Tue January 17 20:57:38 2006
lww/jcfs/109575/SCS200090
Prod#: SCS200090

Nanostructural and Nanomechanical Properties of Synostosed Postnatal Human Cranial Sutures

Nayra Grau, DDS, MS, Joseph L. Daw, MD, DDS, Rupal Patel, BS, Carla Evans, DDS, DMSc, Naama Lewis, BS, Jeremy J. Mao, DDS, PhD

Chicago, Illinois

Craniosynostosis represents a heterogeneous cluster of congenital disorders and manifests as premature ossification of one or more cranial sutures. Cranial sutures serve to enable calvarial growth and function as joints between skull bones. The mechanical properties of synostosed cranial sutures are of vital importance to their function and yet are poorly understood. The present study was designed to characterize the nanostructural and nanomechanical properties of synostosed postnatal sagittal and metopic sutures. Synostosed postnatal sagittal sutures (n = 5) and metopic sutures (n = 5) were obtained from craniosynostosis patients (aged 9.1 ± 2.8 months). The synostosed sutural samples were prepared for imaging and indentation on both the endocranial and ectocranial surfaces with the cantilever probe of an atomic force microscopy. Analysis of the nanotopographic images indicated robust variations in sutural surface characteristics with localized peaks and valleys. In 5 × 5 μm scan sizes, the surface roughness of the synostosed metopic suture was significantly greater (223.6 ± 93.3 nm) than the synostosed sagittal suture (142.9 ± 80.3 nm) (P < 0.01). The Young's modulus of the synostosed sagittal suture at 0.7 ± 0.2 MPa was significantly higher than the synostosed metopic suture at 0.5 ± 0.1 MPa (P < 0.01). These data suggest that various synostosed cranial sutures may have different structural and mechanical characteristics.

Tissue Engineering Laboratory M/C 841, University of Illinois at Chicago, Chicago, Illinois.

This research was supported by USPHS Research Grants DE13964, DE15391, and EB02332, from the National Institute of Dental and Craniofacial Research, and National Institute of Biomedical Imaging and Bioengineering, National Institutes of Health to Dr. Jeremy Mao.

Address correspondence to Dr. Jeremy Mao, Director and Associate Professor, Tissue Engineering Laboratory M/C 841, University of Illinois at Chicago, 801 S. Paulina St., Chicago, IL 60612; E-mail: jmao2@uic.edu.

Key Words: Cranial sutures, synostosis, bone, osteoblast, craniofacial

Cranial sutures are a soft connective tissue interface between mineralized calvarial bones.[1,2] Cranial sutures consist of an array of connective tissue cells such as mesenchymal cells and fibroblast-like cells that proliferate, differentiate, and synthesize extracellular matrices, thus maintaining the presence of suture mesenchyme.[1,2] On the other hand, sutural osteoblasts produce bone matrix, which is mineralized to form skull bones. Longitudinal and expansional growth of cranial bones arrests if cranial sutures undergo either physiologic or pathologic ossification.[1] Craniosynostosis represents a heterogeneous group of congenital disorders that are commonly manifested as premature ossification of one or more cranial sutures. Craniosynostosis is one of the most common craniofacial anomalies and occurs in approximately 1:2,500 live human births. Although more than 150 genetic syndromes have been linked to craniosynostosis, many craniosynostosis cases are nonsyndromic and occur sporadically without apparent association to syndromes. With premature synostosis of cranial sutures, continuing brain growth is believed to result in craniofacial deformities by way of compensatory expansion in the patent sutures. Craniofacial deformities likely result from abnormal intracranial pressure. In addition to craniofacial anomalies, craniosynostosis can manifest as impaired cerebral flow, airway obstruction, impaired vision and hearing, learning difficulties, and adverse psychologic effects.

The causes of craniosynostosis are heterogeneous and not well understood.[3] Despite genetic linkage, such as MSX, FGFR, and TWIST, to several craniosynostosis phenotypes, approximately 50% of craniosynostosis cases likely occur by way of complex functions and interactions of gene products that are subjected to environmental modulations such as mechanical stresses, hematologic or metabolic disorders, and teratogen agents.[3] Despite our increasing understanding of craniosynostosis related genes, little is known about the structural and mechanical properties of synostosed cranial sutures. This is not surprising because little is known about the structural and mechanical characteristics of normal cranial sutures except a few recent attempts.[4–6] The first step toward understanding a biological tissue from an engineering standpoint is to characterize its material properties. The present study was designed to provide some clue of the structural and mechanical properties of synostosed neonatal cranial sutures.

Craniosynostosis may affect any of the cranial sutures in humans, but most commonly involves the sagittal and coronal sutures. Isolated sagittal suture synostosis is most common and accounts for the 57% of the isolated synostosis cases, whereas the isolated coronal suture synostosis accounts for 18% to 24%. It has been speculated that sutural ossification in synostosis starts at one point and spreads along the suture.[7] It is unclear whether synostotic sutural ossification progresses in a random fashion or follows specific patterns, such as in an endocranial-ectocranial and anterior-posterior fashion.[8] Previous work has characterized suture ossification primarily by gross inspections using light microscopy. Microcomputed tomography has also been used to study synostosed sutures at a resolution of 25 μm. Atomic force microscopy (AFM) is a powerful tool to provide reliable micromechanical properties of bone tissue[9] and cranial sutures. This study represents the first known report of using AFM to study the nanomechanical and topographic properties of synostosed sutures.

MATERIALS AND METHODS

Craniosynostotic Patients and Craniofacial Surgery

A total of five synostosed sagittal sutures (n = 5) and five synostosed metopic sutures (n = 5) were obtained during medically necessary suturectomy procedures performed on postnatal patients diagnosed of nonsyndromic craniosynostosis. The average age of the patients with synostosed sagittal suture was 9.2 ± 3.0 months, whereas the average age of the patients with synostosed sagittal suture was 9.0 ± 2.9 months (Table 1). All surgical procedures were performed by one craniofacial and oral and maxillofacial surgeon. The animal protocol was approved by the institutional review board.

Surgical Samples

The synostosed sagittal or metopic sutures, as illustrated in Figure 1A, were dissected aseptically during surgery and immediately placed in 10% paraformaldehyde solution. After the surgeon identified the location of the synostosed suture, small samples of 5 × 3 × 2 mm including both the endocranial and ectocranial surfaces were obtained from each of the synostosed sutures. The ectocranial surface was convex, whereas the endocranial surface was concave. The surgically dissected synostotic suture samples were prepared for microdissection to remove the central region of each synostotic sample for further analysis with AFM. The samples were either scanned fresh with AFM or after placement in a 10% paraformaldehyde solution for temporary storage in a refrigerator at a 4°C. Our previous data have shown that short-term storage in 10% paraformaldehyde did not significantly alter the mechanical properties of sutural samples.

Sample Preparation For Atomic Force Microscopy

The surgically harvested samples were further dissected with a sharp rotation saw (Hall Surgical, Largo, FL). Any remnants of the periosteum or dura mater were removed with care not to cause substantial damage to cortical bone surface using a fine surgical scalpel. The marrow surface of each bone block was rapidly dried and glued onto a glass cover slide using cyanoacrylate. Using a two-sided adhesive tape, the glass cover slide (15 mm in diameter) was fixed to a stainless steel disk, which was magnetically mounted onto the piezoscanner of an AFM. During these procedures, each sample was constantly irrigated with phosphate-buffered saline to prevent dehydration.

Table 1. Distribution of Synostosed Sagittal and Metopic Sutures as well as Patient Age

Synostosed Suture			*Patient Age at the Time of Surgery (months)*			*Mean (months)*
Sagittal	5	11	9	8	13	9.2
Metopic	10	11	11	9	4	9

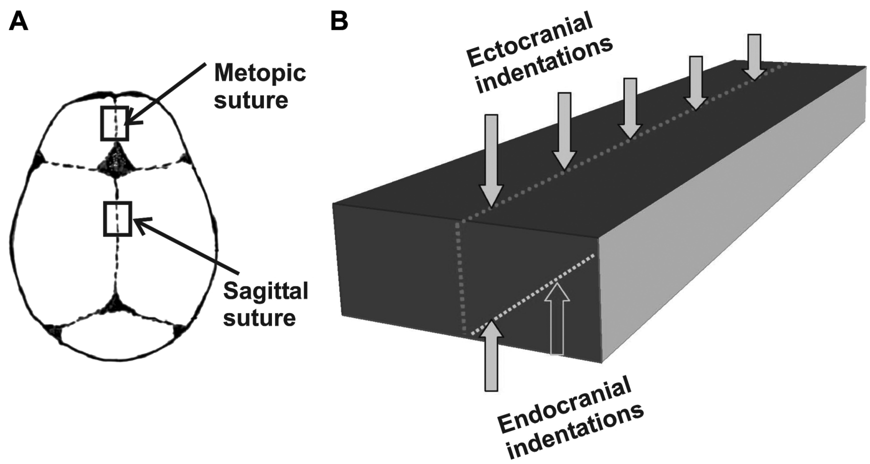

Fig 1 Schematic diagram of the skull and cranial sutures, as well as sample preparation for atomic force microscopy. (A) Superior view of human calvarium. Location of harvested samples of synostosed metopic and sagittal sutures in rectangular boxes. (B) Diagram of isolated sutural specimen with an overall dimension of 5 × 3 × 2 mm^3. Superior surface represents the ectocranial surface, whereas inferior surface represents endocranial surface. Downward and upward arrows are locations of scanning and indentation with atomic force microscopy. The dotted line is location of the suture.

Nanoscopic Imaging and Nanoindentation with Atomic Force Microscopy

A total of five regions of each synostosed suture were scanned on each of ectocranial and endocranial surfaces (Fig 1B) using an AFM (Nanoscope IIIa, Veeco-Digital Instruments, Santa Barbara, CA). Each region was separated from the next by 1 mm. Upon nanoindentation, both topographic and force spectroscopy images were obtained using contact-mode AFM. An oxide-sharpened silicone nitride, $Si_3N_{4,}$ scanning tip,was used for both topographic and nanoindentation imaging with a nominal force constant of $k = 0.12$ Nm and a radius of tip curvature of 20 nm. The scan size was 5·5 μm, and scan rates were 1 Hz for topographic imaging and 14 Hz for force volume imaging. Upon satisfactory topographic imaging, the spectroscopy data were mapped in an image in which load and nanoindentation in the Z plane were captured. For each force spectroscopy scan, the average Young's modulus (E) was calculated from individual calculations of 10 centrally located points using the Hertz model[10,11] as shown in equation 1 below:

$$E = \frac{3F(1 - v^2)}{4\sqrt{R}\delta^{3/2}} \qquad (1)$$

where E is the Young's modulus, F is the applied nanomechanical load, ν is the Poisson's ratio, R is the radius of probe tip curvature, δ is the amount of nanoindentation. Nanoindentation force (F) was calculated using the equation $F = k \cdot d$, where k is the spring constant of the cantilever ($k = 0.12$ N·m) and d is the cantilever deflection distance on indentation. The Poisson ratio was assumed to be 0.30 for bone.[12]

Topographic images of 5·5 μm were obtained for some, but not all, samples. Surface roughness (R_a) for both the ectocranial and endocranial surfaces was obtained using equation 2 as follows:

$$R_a = \frac{\sum_{i=1}^{N} |Z_i - Z_{cp}|}{N} \qquad (2)$$

where Z_{cp} is the Z value of the center plane, Z_i is the current Z value, and N is the number of points within a given area. For R_a analysis, height images of all samples were obtained. The regions for R_a analysis were 5·5 μm.

Statistical Analysis

The average E and R_a were analyzed using Student's *t*- tests. A P value of less than 0.05 was considered of statistical significance.

RESULTS

Nanoscopic imaging and nanoindentation revealed interesting characteristics of the synostosed postnatal sagittal and metopic sutures. At 5 × 5 μm scan sizes with AFM, the synostosed sagittal suture on both the endocranial and ectocranial surfaces demonstrated multiple localized peaks and valleys (Fig 2). Close examination of the peaks and valleys indicated that surface topographic variation was within 1,000 nm (Fig 2). Qualitatively, topographic features of the synostosed metopic suture were more robust, showing multiple localized peaks and valleys with height variations up to 1,500 nm (Fig 3). These qualitative observations were confirmed by the quantification of the mean R_a. The R_a

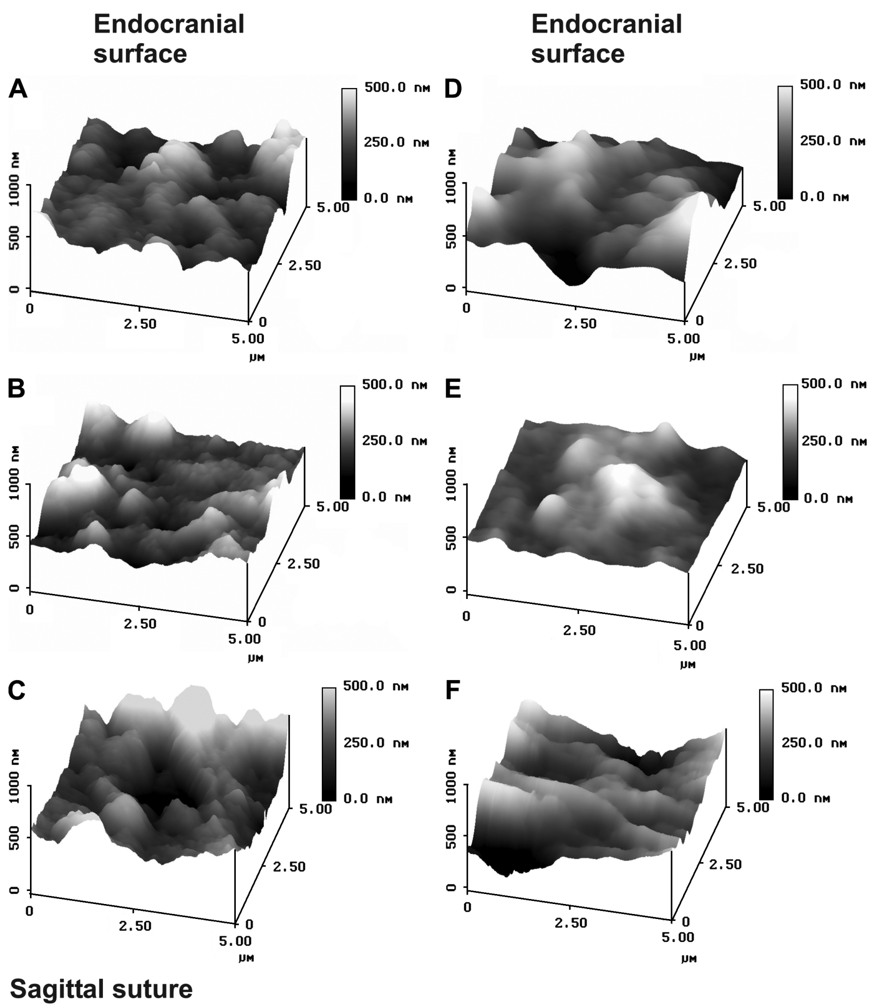

Fig 2 Representative topographic images of synostosed sagittal suture. Topographic images of the endocranial surface are illustrated at left column (A, B, C), whereas topographic images of the ectocranial surface are illustrated at right column (D, E, F). Multiple peaks and valleys represent surface microstructures on the endocranial and ectocranial surfaces of the synostosed sagittal suture. Note that the variation of surface topography was up to 1,000 nm.

of the synostosed metopic suture at 223.6 ± 93.3 nm was significantly greater than the mean R_a of the synostosed sagittal suture at 142.9 ± 80.3 nm ($P < 0.01$) (Fig 4A). However, there was a lack of statistical significance in the mean R_a between the endocranial surface (201.9 ± 123.4 nm) and the ectocranial surface (201.2 ± 74.8 nm) of the synostosed metopic suture. Similarly, the mean R_a between the endocranial surface (136 ± 119.9 nm) and the ectocranial surface (147.6 ± 42.7 nm) of the synostosed sagittal suture also lacked significant differences.

Typical force-volume images depicted the deflection of the AFM scanning tip at given Z positions from which force plots were selected for the endocranial and ectocranial surfaces of the synostosed sagittal and metopic sutures (Fig 5). Nanoelastic data collected from force spectroscopy images on nanoindentation demonstrated notable differences between the synostosed sagittal suture (Fig 5, A and B) and the synostosed metopic suture (Fig 5, C and D). Analysis of force-volume images of the elastic maps of synostosed sagittal and metopic sutures in Figure 5 yielded the E, which represent the mechanical properties of the synostosed sutures. The mean E for the synostosed sagittal suture at 0.7 ± 0.2 MPa was significantly greater than the mean E for the synostosed metopic suture at 0.5 ± 0.1 MPa ($P < 0.01$) (Fig 4B). However, the differences in the average E between the ectocranial and endocranial surfaces lacked statistical significance for either the synostosed sagittal or metopic suture.

Discussion

The present study represents an original investigation of the physical properties of synostosed cranial sutures in early human childhood. The physical properties of cranial sutures have been difficult to study with conventional mechanical testing approaches because of the microscopic dimension of

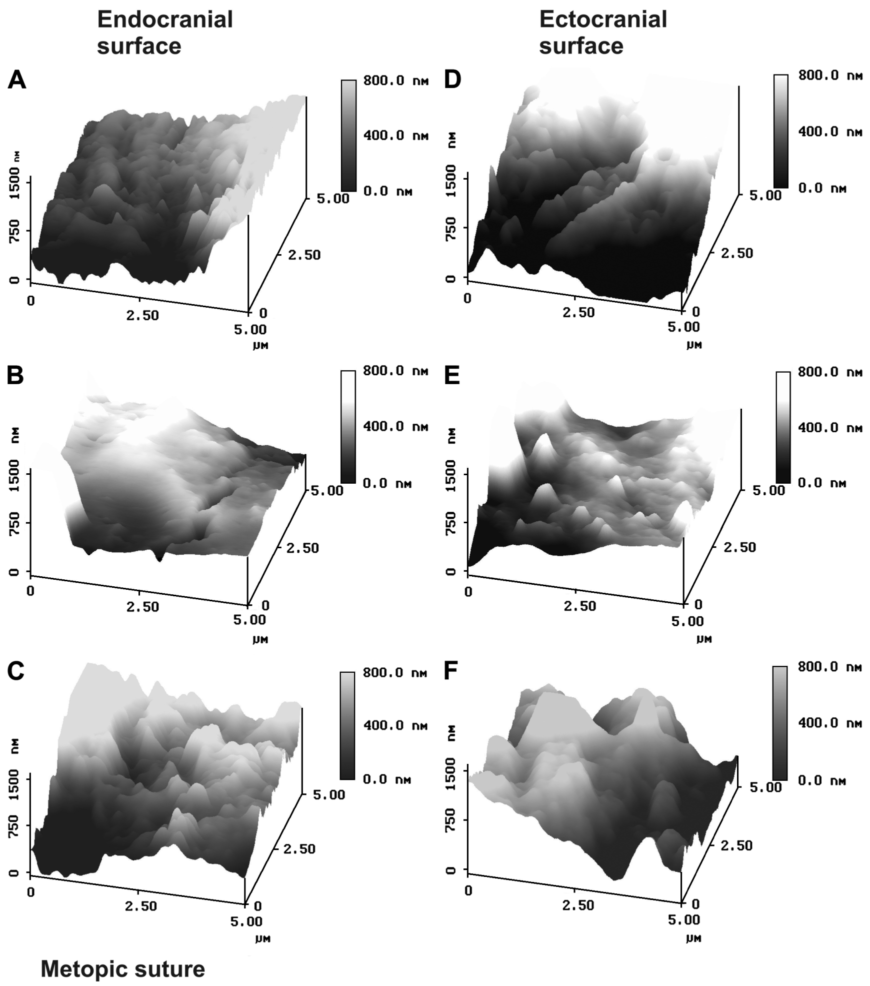

Fig 3 Representative topographic images of synostosed metopic suture. Topographic images of the endocranial surface are at left column (A, B, C), whereas topographic images of the ectocranial surface are at right column (D, E, F). Multiple peaks and valleys represented surface microstructures on the endocranial and ectocranial surfaces of the synostosed metopic suture. Note that the variation of surface topography was up to 1,500 nm.

cranial sutures. After previous investigations of nanoscale structures by physical scientists, AFM has been recently used by biomedical scientists to investigate the molecular, cellular, and tissue structures. The present study is a continuation of our ongoing investigations of skeletal tissues using AFM.[11,13] In our previous studies, AFM was used as a nanoindentation device for measuring the physical properties of articular cartilage, chondrocyte matrices, cranial sutures, and sutural mineralization front.

Examination of the topographic images reveals variations of cranial suture surfaces with multiple randomly localized peaks and valleys. These peaks and valleys likely reflect an irregular bone mineralization pattern in both the endocranial and ectocranial surfaces. The localized variations in surface topography are perhaps consistent with the observation of multiple mineralized nodules in synostosed cranial sutures.[14] In the present work, the endocranial and ectocranial surfaces of the synostosed metopic sutures showed rougher and more irregular topographic features than the synostosed sagittal suture. This can probably be accounted for by the following factors. Because of its anatomic location, the metopic suture is highly influenced by the masseter muscle. This is indirectly supported by a greater tensile strain in the anterior portion of the interfrontal suture in a pig model.[15] The surfaces of the synostosed metopic sutures may increase their structural complexity in response to mechanical stresses transmitted to the suture. Second, mechanical stresses from masticatory forces transmitted to the sagittal suture may be offset by mechanical stresses generated from the contraction of the bilateral temporalis muscles. Clearly, the temporalis muscle has an opposing effect to the masseter muscle.[15,16] Although the magnitude of masticatory and muscular forces are small in infants, the resultant mechanical stresses transmitted to postnatal cranial sutures is anticipated

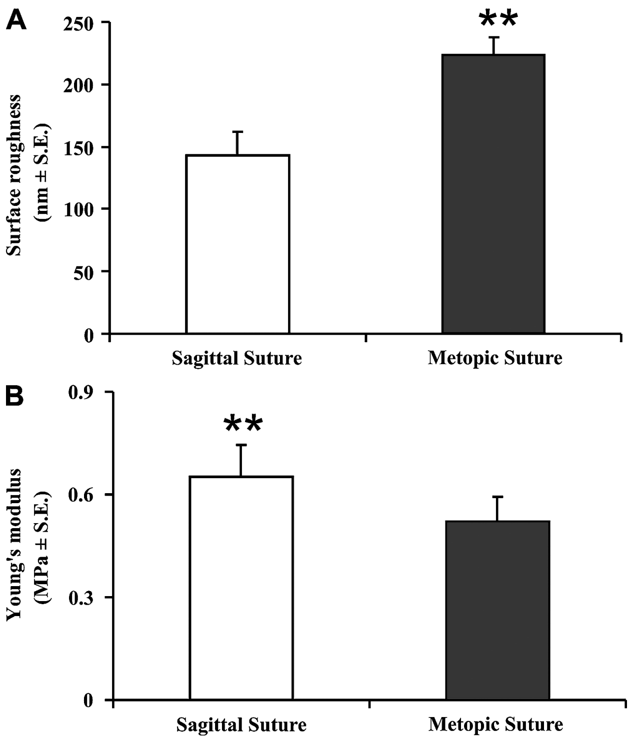

Fig 4 Quantification of surface topography and Young's moduli of the synostosed sagittal and metopic sutures. (A) Histograms of mean surface roughness (R_a) of synostosed sagittal and metopic sutures (**$P < 0.01$). (B) Histograms of Young's moduli (E) of synostosed sagittal and metopic sutures (**$P < 0.01$).

to be sufficient to induce metabolic changes.[1] Mechanical stresses in cranial sutures may regulate the apparently low level of mineralization of synostosed cranial sutures.[14] The age range of the patients from whom the synostosed sutural samples were obtained was 4 to 13 months. Cranial sutures are less stiff and less mineralized than surrounding bone.[17] From the patient's age and the current mechanical data, it appears that the synostosed infant sutures are not nearly as stiff as fully mineralized adult bone. Third, although both the sagittal and metopic sutures are midline sutures with presumably similar roles in craniofacial growth, the timing of physiologic fusion differs drastically between these two sutures. The human metopic suture physiologically undergoes osseous fusion at approximately 3 months after birth,[18] whereas the sagittal suture begins to undergo ossification at 22 years of age. It is probable that there is less time for establishing surface structural complexity in the metopic suture than the sagittal suture.

The present finding of lower E and higher R_a in the metopic suture than the sagittal suture can also be related to a previous study.[19] Bone in the mineralizing regions of the synostosed suture has lower mineralization than adjacent sutural bone and more osteoblasts lining the trabeculae, in addition to lower trabecular density and thickness.[19] These morphologic features associated with synostosed cranial sutures appear to explain the higher R_a of the metopic suture and the increased porosity and low mineralization correlate with a lower E associated with the synostosed metopic suture. Metopic suture closure may involve chondroid tissue. In contrast, growth of the sagittal suture appears to rely solely on bone apposition. The different mechanisms by which these sutures ossify may also account for the presently observed differences in their E and R_a.

Despite significant differences in R_a between the sagittal and metopic sutures as identified in the current study, there is a lack of significant differences in either the average R_a or average E between the endocranial and the ectocranial surface of either the metopic or sagittal suture. This lack of statistically significant differences in E and R_a between the endocranial and ectocranial surfaces may be attributed to the possibility that the currently studied synostosed sutures are from postnatal human samples with age ranges from 4 to 13 months. An animal model is probably warranted to investigate the endocranial and ectocranial surfaces of synostosed sutures at an embryonic stage so that the initial phases of mineralization can be subjected to nanoindentation.

The present work has the following caveats. First, the human synostosed samples are heterogeneous and limited in regard to sample size and age range. These likely have contributed to the observed variation in both nanostructural and nanomechanical data. Second, the AFM used as a nanoindenter can only probe the synostosed sutural surface instead of the inner portion of the synostosed suture. Although the mechanical properties of synostosed sutures perpendicular to the ecto- and endocranial surfaces are important for the understanding of sutural physical properties, other techniques, such as magnetic resonance or elastomicrography, may help illustrate the mechanical properties of synostosed sutures in the central core of the bone. Within the constraints of these caveats, the present data represent the first demonstration of differences in surface microscopic characteristics and mechanical properties between two synostosed cranial sutures. In comparison with accumulating focus on the genetics and molecular biology of craniosynostosis, improvement in

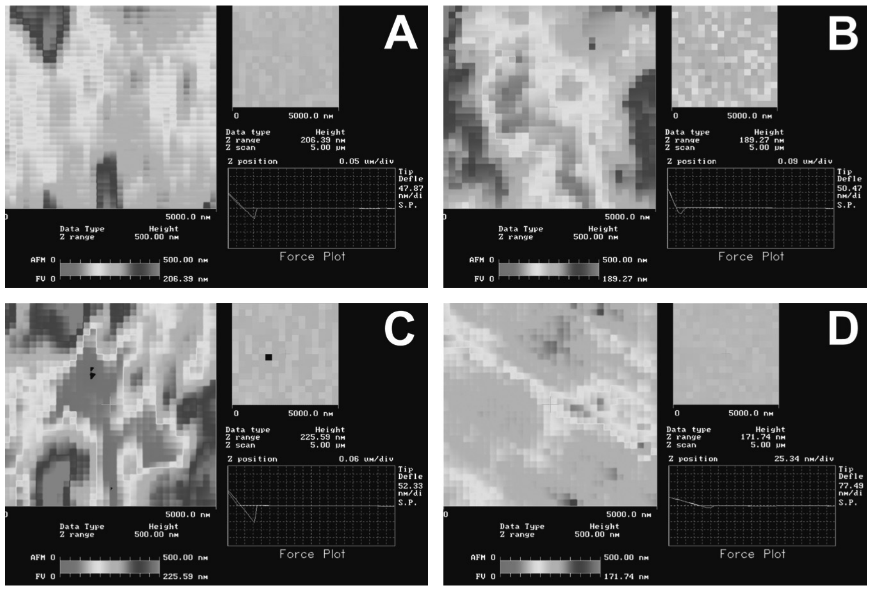

Fig 5 Force volume images and force plots of a synostosed sagittal and metopic suture samples. (A) Representative image of endocranial surface of a synostosed sagittal suture. (B) Representative image of ectocranial surface of a synostosed sagittal suture. (C) Representative image of endocranial surface of a synostosed metopic suture. (D) Representative image of ectocranial surface of a synostosed metopic suture. In each subfigure, the elastic map in the larger square was height image with colors coded to relative surface elevations, whereas smaller square contained a force-volume image mapping atomic force microscope cantilever tip-sample interactions. Force plot represents tip-sample interaction at a given location. In force plot, X-axis represents vertical position of piezostage on which the sample was mounted. Y-axis represents vertical position of cantilever tip relative to a vertical deflection set point. Yellow line represents interaction between cantilever tip and sample.

our understanding of the physical properties of synostosed cranial suture undoubtedly would help clinicians to further understand the pathogenesis of craniosynostosis.

The experimental work described in this manuscript is from the Master of Science thesis research by Nayra Grau. The authors thank Grace Viana for performing statistical analysis. The authors thank Aurora Lopez for general technical assistance.

REFERENCES

1. Mao JJ. Mechanobiology of craniofacial sutures. J Dent Res 2002;81:810–816
2. Opperman LA. Cranial sutures as intramembranous bone growth sites. Dev Dyn 2000;219:472–485
3. Wilkie AOM, Morriss-Kay GM. Genetics of craniofacial development and malformation. Nature 2001;2:458–468
4. Margulies SS, Thibault KL. Infant skull and suture properties: measurements and implications for mechanisms of pediatric brain injury. J Biomech Eng 2000;122:364–371
5. McLaughlin E, Zhang Y, Pashley D, Borke J, Yu J. The load-displacement characteristics of neonatal rat cranial sutures. Cleft Pal Craniofac J 2000;37:590–595
6. Tanaka E, Miyawaki Y, del Pozo R, Tanne K. Changes in the biomechanical properties of the rat interparietal suture incident to continuous tensile force application. Arch Oral Biol 2000;45: 1059–1064
7. Albright AL, Byrd RP. Suture pathology in craniosynostosis. J Neurosurg 1981;54:384–387
8. Moursi AM, Winnard PL, Fryer D, Mooney MP. Delivery of transforming growth factor-β2-perturbing antibody in a collagen vehicle inhibits cranial suture fusion in calvarial organ culture. Cleft Palate Craniofac J 2003;40:225–232
9. Hengsberger S, Kulik A, Zysset P. A combined atomic force microscopy and nanoindentation technique to investigate the elastic properties of bone structural units. Eur Cells Mats 2001;1:12–17
10. Heinz WF, Hoh JH. Spatially resolved force spectroscopy of biological surfaces using the atomic force microscope. Trends Biotechnol 1999;17:143–150
11. Radhakrishnan P, Lewis NL, Mao JJ. Zone-specific micromechanical properties of the extracellular matrices of growth plate cartilage. Ann Biomed Eng 2004;32:284–291
12. Kysset PK, Guo XE, Hoffler CE, Moore KE, Goldstein SA. Elastic modulus and hardness of cortical and trabecular bone measured by nanoindentation in the human femur. J Biomech 1999; 32:1005–1012
13. Patel RV, Mao JJ. Microstructural and elastic properties of the extracellular matrices of the superficial zone of neonatal articular cartilage by atomic force microscopy. Front Biosci 2003;8: a18–a25
14. Shevde NK, Bendixen AC, Maruyama M, Li BL, Billmire DA. Enhanced activity of osteoblast differentiation factor (PEBP2aa/CBFa1) in affected sutural osteoblasts from patients with non-syndromic craniosynostosis. Cleft Palate Craniofac J 2001;38:606–614
15. Herring SW, Teng S. Strain in the braincase and its sutures during function. Am J Phys Anthrop 2000;112(575):593

16. Mao JJ, Wang X, Kopher RA. Suture biomechanics: implications on craniofacial orthopedics. Angle Orthod 1999;73:128–135
17. Jaslow CR. Mechanical properties of cranial sutures. J Biomech 1990;23:313–321
18. Vu HL, Panchal J, Parker EE, Levine NS, Francel P. The timing of physiologic closure of the metopic suture: a review of 159 patients using reconstructed 3D CT scans of the craniofacial region. J Craniofac Surg 2001;12:527–532
19. Ozaki W, Buchman S, Muraszko K, Coleman D. Investigation of the influences of biomechanical force on the ultrastructure of human sagittal cranyosynostosis. Plast Reconst Surg 1998; 102:1385–1394

Invited Discussion

Re: Nanostructural and Nanomechanical Properties of Synostosed Postnatal Human Cranial Sutures. Grau et al., J Craniofac Surg 2005;16:000—000.

Early expansion of the skull is facilitated by appositional bone formation at patent cranial sutures. Predominantly adaptable centers that respond to extrinsic biomechanical signals, sutures permit allometric growth of the calvarial vault.[1] Although several studies have articulated a strong association between growth of the brain and adjacent skull, how the intervening mesenchyme and osteogenic fronts between the overlying bony plates fundamentally respond to forces remain largely unknown.[2,3] Only recently have investigators begun to elucidate the complex interrelationship between strain and cranial suture development, but much of our knowledge regarding fundamental structural characteristics must still be defined.[2,4–6] As the authors of this work elaborate, a plausible first step toward a more complete understanding of the biomechanical properties would be a detailed description of material properties. By analyzing the nanomechanical and topographic properties of synostosed sutures, the authors potentially provide an insight into the process of abnormal fusion and may likewise suggest a novel avenue to the study of craniosynostosis.

This study by Grau et al endeavored to characterize the nanostructural and nanomechanical properties of synostosed sagittal and metopic sutures. Five prematurely fused metopic and sagittal sutures were obtained from children with nonsyndromic craniosynostosis undergoing surgical correction. After removal of periosteum and dura mater, the central region of each sample was prepared for analysis using an atomic force microscope. The surface of each synostosed suture was characterized by nanoindentation, and force spectroscopy was used to determine the sample's structural properties. An average surface roughness was calculated along with a Young's modulus to describe material stiffness. Nanoscopic imaging demonstrated a qualitatively complex topography for the fused metopic suture, spanning a range of up to 1,500 nm between adjacent peaks and valleys. The synostosed sagittal suture comparatively demonstrated far less variability, with a calculated mean surface roughness statistically less than that in the metopic suture. These findings persisted irrespective of investigations on either the endocranial or ectocranial surface. Nanoelastic data obtained from force spectroscopy revealed a compelling difference in the structural properties between the metopic and sagittal suture samples. Estimated Young's moduli, describing the relationship between stress and strain, was significantly greater in the fused sagittal sutures. Further analysis demonstrated no statistical intrasutural difference between the endocranial and ectocranial surface for each sample set. Considering these data, the authors speculate that differences observed may, in part, be the result of anatomic location and its accompanying masticatory forces. With metopic sutural development presumably regulated by masseteric activity, the increased tensile strain, as the authors argue, may contribute to both enhanced topographic complexity and decreased stiffness.

The application of atomic force microscopy to the study of synostosed sutures represents an innovating approach for investigations on resultant biomechanical properties of premature fusion. As the authors mention, conventional approaches to mechanical testing have been limited by the microscopic dimension of cranial sutures. But although characterization of synostosed sutures remains intriguing, a more salient consideration to be made is how the native suture complex develops in response to stress. Masticatory hypofunction has been one approach taken to investigate the influence of extrinsic stress on development of the craniofacial skeleton.[4,7] Anthropometric measurements made on rats fed a powdered diet revealed no differences in cranial growth when compared with animals fed hard pellets.[7,8] Furthermore, studies have demonstrated development and growth of sutures in the absence of any muscle activity.[4] By transplanting whole infant rat heads to the body of isohistogeneic adults, Hirabayashi et al[4] were able to completely dissociate craniofacial development from masticatory activity. Using this model, sutural development was observed to not only befall, but to also play an active role, in growth.[4] Initial suture patterning therefore proceeds despite withdrawal of extrinsic influences.[4,7,8] Whether diminished or entirely absent, strain induced by muscle activity does not clearly contribute to early suture specification.

Although the data have demonstrated a relative independence of initial suture development and growth, subsequent maturation and refinement of cranial sutures has been increasingly linked to extrinsic force exposure.[6,9–11] As early as 1957, Moss[12] purported that the fine details of suture morphology was a consequence of responses to applied strain. Mechanical isolation of sutures with methyl-2-cyanoacrylate diminished osteogenesis when analyzed both radiographically and histologically.[10] In work done by Kopher and Mao,[9] suture response to both cyclic and static force was assessed after 12 days of maxillary loading. Interestingly, in the presence of extrinsic oscillatory strain, sutures were observed to develop greater widths when compared with either static applied strain or sham controls.[9] Histologic analysis demonstrated a significant increase in mesenchymal cellularity, and fluorescent labeling revealed an elevated rate of osteogenesis when sutures were exposed to cyclic force.[9] These studies demonstrate a clear adaptive response to extrinsic mechanical stress.[9–11] In the absence of masticatory forces, the intricate details of suture specification may thus be lost.

The work by Grau et al appreciably contributes to our understanding of the biomechanical properties of synostosed sutures. But although the authors have demonstrated a significant difference in material properties for fused metopic and sagittal sutures, they only begin to address the fundamental interrelationship between stress and suture development. Recent studies have clearly demonstrated suture specification to occur in the absence of masticatory hypofunction; fine details of suture morphology, however, rely profoundly on exposure to extrinsic forces.[7,9–11] In integrating these findings, sutures appear to be adaptable centers of growth capable of responding to variations in mechanical environment.[9,11] The data in this present work accentuate this notion, with divergent topography and stiffness a likely culmination of differences in masticatory stress. How this ultimately influences sutural fate, however, remains as the central question to be answered as we strive to better understand in what manner forces may ultimately result, or at the very least, contribute, to premature suture fusion.

Derrick C. Wan, MD
Julia C. Chen
Michael T. Longaker, MD, MBA
Department of Surgery
Division of Plastic and Reconstructive Surgery
Children's Surgical Research Program
Stanford University School of Medicine
Stanford, California

References

1. Warren SM, Greenwald JA, Spector JA, et al. New developments in cranial suture research. Plast Reconstr Surg 2001;107:523–540
2. Mao JJ. Mechanobiology of craniofacial sutures. J Dent Res 2002;81:810–816
3. Rafferty KL, Herring SW. Craniofacial sutures: Morphology, growth, and in vivo masticatory strains. J Morphol 1999;242:167–179
4. Hirabayashi S, Harii K, Sakurai A, et al. An experimental study of craniofacial growth in a heterotopic rat head transplant. Plast Reconstr Surg 1988;82:236–243
5. Behrents RG, Carlson DS, Abdelnour T. In vivo analysis of bone strain about the sagittal suture in macaca mulatta during masticatory movements. J Dent Res 1978;57:904–908
6. Sun Z, Lee E, Herring SW. Cranial sutures and bones: Growth and fusion in relation to masticatory strain. Anat Rec A Discov Mol Cell Evol Biol 2004;276:150–161
7. Ulgen M, Baran S, Kaya H, et al. The influence of the masticatory hypofunction on the craniofacial growth and development in rats. Am J Orthod Dentofacial Orthop 1997;111:189–198
8. Katsaros C, Berg R, Kiliaridis S. Influence of masticatory muscle function on transverse skull dimensions in the growing rat. J Orofac Orthop 2002;63:5–13
9. Kopher RA, Mao JJ. Suture growth modulated by the oscillatory component of micromechanical strain. J Bone Miner Res 2003;18:521–528
10. Foley WJ, Kokich VG. The effects of mechanical immobilization on sutural development in the growing rabbit. J Neurosurg 1980;53:794–801
11. Henderson JH, Longaker MT, Carter DR. Sutural bone deposition rate and strain magnitude during cranial development. Bone 2004;34:271–280
12. Moss ML. Experimental alteration of sutural area morphology. Anat Rec 1957;127:569–589